SCIENTIFIC REPORTS

OPEN

SUBJECT AREAS:
MATERIALS SCIENCE
MATERIALS FOR ENERGY AND CATALYSIS
SOLID-STATE CHEMISTRY
PHOTOCATALYSIS

Received
25 November 2012

Accepted
30 April 2013

Published
16 May 2013

Correspondence and requests for materials should be addressed to Q.Z. (qczhang@ntu.edu.sg)

# Molecule-Based Water-Oxidation Catalysts (WOCs): Cluster-Size-Dependent Dye-Sensitized Polyoxometalates for Visible-Light-Driven $O_2$ Evolution

Junkuo Gao[1], Shaowen Cao[1], Qiuling Tay[1], Yi Liu[1], Lingmin Yu[1], Kaiqi Ye[1], Peter Choon Sze Mun[1], Yongxin Li[2], Ganguly Rakesh[2], Say Chye Joachim Loo[1], Zhong Chen[1], Yang Zhao[1], Can Xue[1] & Qichun Zhang[1]

[1]School of Materials Science and Engineering, Nanyang Technological University, Singapore 639798, Singapore, [2]School of Physical and Mathematical Sciences, Nanyang Technological University, Singapore 637371, Singapore.

**From atomic level to understand the cluster-size-dependant behavior of dye-sensitized photocatalysts is very important and helpful to design new photocatalytic materials. Although the relationship between the photocatalytic behaviors and particles' size/shape has been widely investigated by theoretical scientists, the experimental evidences are much less. In this manuscript, we successfully synthesized three new ruthenium dye-sensitized polyoxometalates (POM-n, n relate to different size clusters) with different-sized POM clusters. Under visible-light illumination, all three complexes show the stable $O_2$ evolution with the efficient order POM-3 > POM-2 > POM-1. This cluster-size-dependent catalytic behavior could be explained by the different numbers of M = $O_t$ (terminal oxygen) bonds in each individual cluster because it is well-known that Mo = $O_t$ groups are the catalytically active sites for photooxidation reaction. The proposed mechanism of water oxidation for the dye-sensitized POMs is radical reaction process. This research could open up new perspectives for developing new POM-based WOCs.**

Visible-light-driven photocatalysts are very attractive because they could be one of the most promising methods to solve the energy problem and effectively reduce environmental contamination[1–8]. The photocatalytic behaviors strongly depend on atomic configuration, band gap positions, size, shape, and surface reactivity. Recent evidence in $TiO_2$ catalysts has already shown that the facet effect is one of key factors to determinate the photocatalytic reactivity because the adsorption/desorption of molecules and photoexcited electrons transfer are extremely sensitive to surface structure states[9–11]. However, as another important factor, size-dependent photocatalytic behavior has received much less attention. Although some groups has already shown that certain sizes of nanoparticles might be the key for achieving the high photocatalytic activity from both experimental and theoretical studies, a direct experimental understanding on size-dependent photocatalytic behaviors at atomic scale is unprecedented[12–15]. This gap in knowledge strongly motivates us to carry out our research on molecule-based water-oxidation-catalysts (WOCs): cluster-size-dependent dye-sensitized polyoxometalates for visible light driven $O_2$ evolution.

Currently, the widely studied photocatalyst system is metal oxides because of their diverse compositions, high stability, high efficiency, and the possibility of overall water splitting[16–20]. As one branch of metal oxides, polyoxometalates (POMs) -- attractive anionic transition metal nanoclusters, exhibit interesting structural diversity and exceptional physical properties[21–24]. Especially, their nanosized geometry, unique optical and electronic properties as well as excellent chemical reactivity make them the promising candidates for photocatalytic $H_2$ and $O_2$ evolution[25–30].

Since the sun emits its maximum flux of photons in visible region, the photocatalytic efficiency will be dramatically enhanced if the photocatalytic reactions could be driven by visible light[31]. Unfortunately, most POMs show no or very little absorption in the visible region[32–34]. It is necessary to extend their absorption by

introducing light harvesting component (or photosensitizer) into POMs. There are two ways to realize this purpose: (1) using inorganic components such as cobalt oxides, ruthenium oxides, copper oxides, or even gold nanoparticles because these materials have diverse colors; and (2) employing metal-organic complexes (e.g. tris(1,10-phenanthroline) ruthenium ($[Ru(phen)_3]^{2+}$) or pure organic dyes (e.g. methyl viologen, methylene blue) because cationic dyes can act as charge-balancing ions[31,35]. In this research, we are interested in introducing ruthenium complexes into POMs because ruthenium chromophores have been wildly used in photocatalysis, water splitting, and dye-sensitized solar-cell devices[36–39]. Although *in-situ* formed organic-inorganic hybrid complexes between POMs and ruthenium chromophore photosensitizers have been demonstrated as visible-light-driven photocatalysts for oxygen evolution[40–42], the full understanding of their structure-reactivity relationship and oxidation mechanism seems not to be fully achieved.

Here, we go further to explore cluster-size-dependent dye-sensitized polyoxometalate clusters at atomic level and aim to understand the relationship between cluster sizes and photocatalytic behaviors. Three novel POMs-ruthenium photosensitizer hybrid complexes (denoted as **POM-n**, n = 1,2,3) have been synthesized and fully characterized through single-crystal X-ray diffraction analysis and other tools. In addition, their visible-light-driven water-oxidation behaviors have also been investigated and the corresponding oxidation mechanism has been studied via both experimental and theoretical methods. Our results provide solid evidence that the cluster sizes in **POM-n** complexes did affect their photocatalytic behaviors.

## Results

All compounds were synthesized either by solution process at room temperature or under solvothermal conditions at 110°C. The starting materials $(TBA)_2[Mo_6O_{19}]$ and α-$(TBA)_4[Mo_8O_{26}]$ were prepared according to the literature procedure[43,44]. **POM-1** ($[Ru(C_{12}N_2H_8)_3CH_3OH][Mo_6O_{19}]$) was obtained as orange-red crystals in 10 days by slow diffusion of methanol solution of dichlorotris(1,10-phenanthroline) ruthenium (II) hydrate into DMF solution of $(TBA)_2[Mo_6O_{19}]$. **POM-2** and **POM-3** were synthesized under solvothermal conditions with α-$(TBA)_4[Mo_8O_{26}]$ and dichlorotris(1,10-phenanthroline) ruthenium (II) hydrate as starting materials. For **POM-2**, additional starting material sulfur is required. The structures were determined from single-crystal X-ray diffraction data collected on APEX II CCD diffractometer.

The crystal structure analysis of **POM-n** reveals that these materials are made of anionic POM clusters and charge-balancing cations tris(1,10-phenanthroline) ruthenium ($[Ru(phen)_3]^{2+}$. All **POM-n** crystallized in triclinic space group *P*-1. The asymmetric unit for **POM-1** is constituted of a Linqvist anion, one $Ru(phen)_3^{2+}$ chromophore cation, and a methanol molecule (Figure 1a), while **POM-2** has one Strandberg-type heteropolyanion $[Mo_5S_2O_{23}]^{4-}$, one $Ru(phen)_3^{2+}$ cation, two $[NH_2(CH_3)_2]^+$ species from the decomposition of DMF (Figure 1b), one $H_2O$ molecule, and one DMF molecule. As to **POM-3**, it is made by one α-$[Mo_8O_{26}]^{4-}$ anion, two $Ru(phen)_3^{2+}$ cations, and one acetonitrile molecule (Figure 1c). Details of the crystal structure and refinement data are provided in supporting information (Supplementary Table S1). The IR spectra (Supplementary Fig. S1) and experimental powder XRD patterns for

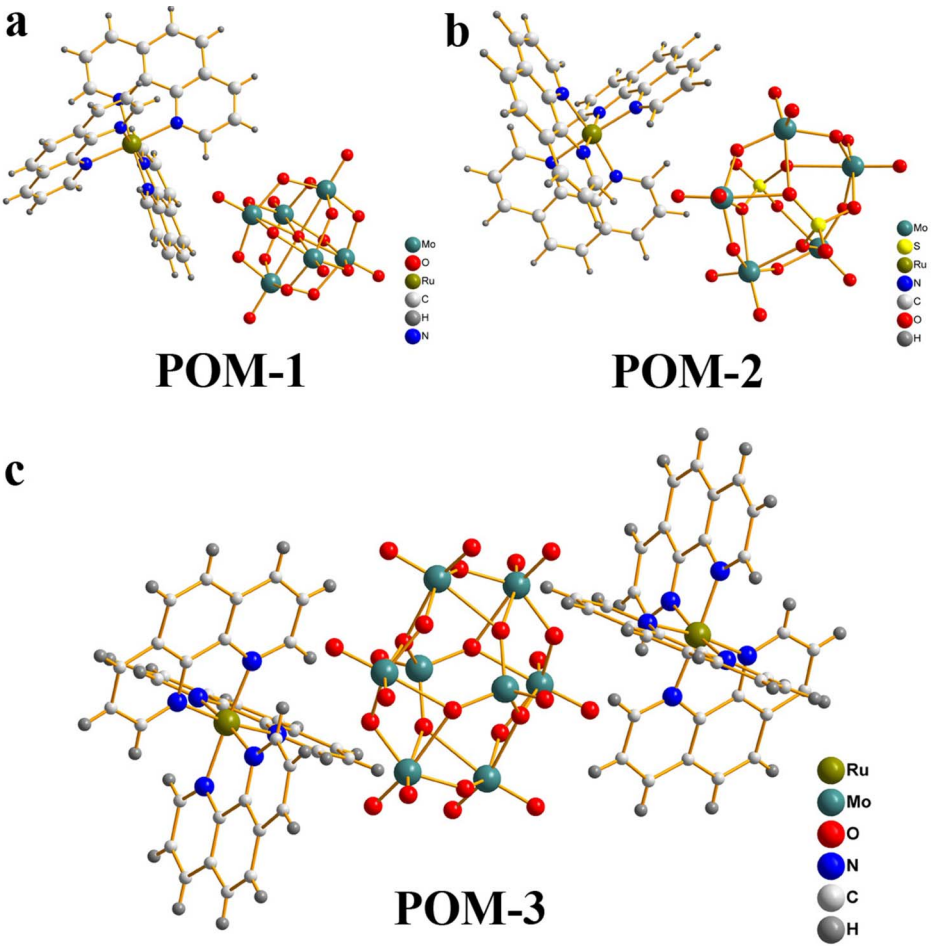


**Figure 1 | The structures of hybrid materials POM-1–3.**

**POM-n** (Supplementary Fig. S2–S4) confirmed the phase purity of the bulk materials of **POM-1** ~ **3**.

The diffuse reflectance spectra were recorded on a PerkinElmer Lambda 750 s UV-Vis spectrometer. As shown in Figure 2, the spectra of **POM-1**, **POM-2**, and **POM-3** show a broad range of absorption in the visible range from ~400 nm to 600 nm. The absorption onsets occur at about 618 nm for **POM-1**, 587 nm for **POM-2** and 601 nm for **POM-3**, which suggests that the band gaps of **POM-1**, **POM-2**, and **POM-3** are 2.01 eV, 2.11 eV and 2.06 eV, respectively. For comparison, UV-Vis absorption of the starting material $Ru(phen)_3Cl_2$ were also measured. Since the absorptions of all individual clusters Mo5, Mo6, and Mo8 are less than 400 nm[45–47], the dramatically-red-shift absorptions hint that **POM-n** could be good candidates as visible-light-driven photocatalysts.

The density of states (DOS) and electronic band structures of **POM-1**, **POM-2** and **POM-3** are calculated using the density functional theory (DFT) in CASTEP program[48]. The calculated energy gaps for **POM-1**, **POM-2** and **POM-3** are 1.27 eV, 1.83 eV, and 1.71 eV, respectively. Although the theoretical calculation results gave relatively lower band gaps comparing with the experimental data, the band gap values (**POM-2** > **POM-3** > **POM-1**) displayed the same trend as experimental values. As depicted in Supplementary Fig. S5–S10, valence bands (VBs) of all three POM complexes near the Fermi level (from −0.5 eV to 0.0 eV) are mainly contributed from the *d* orbitals of Ru atom in the $Ru(phen)_3^{2+}$ part. The VBs spreading from −2.0 eV to −0.5 eV are mainly constituted of the Mo-oxo clusters. The conduction bands (CBs) above the Fermi energy are mostly made up of the $Ru(phen)_3^{2+}$ sensitizer part. The characteristic of band structures indicated that after removing an electron away from the POM complexes via photo-excitation, a hole will be generated on the orbitals of Ru atom. The small energy gaps between the Ru and Mo-oxo clusters in VBs that close to the Fermi energy make the hole transfer to the Mo-oxo clusters possible by capturing electron from the photo-excited Mo-oxo clusters to the reduced $Ru^{3+}$ atom. The holes located in Mo-oxo clusters could be used to oxidize water molecules, making the POM complexes as potential WOCs, which will be further studied via photocatalytic experiments.

The catalytic activity for water oxidation of all compounds was investigated by using typical photocatalytic setup with $Na_2S_2O_8$ as sacrificial electron acceptor. All three photosensitizer-POM complexes act as heterogeneous water oxidation catalysts since they are not soluble in water. Note that there is no $O_2$ evolution happening when the blank solution (only containing the $Ru(phen)_3Cl_2$ and $Na_2S_2O_8$) are illuminated under visible light ($\lambda > 420$ nm). Also, when only the starting materials $(TBA)_2[Mo_6O_{19}]$ and $\alpha$-$(TBA)_4[Mo_8O_{26}]$ and sacrificial reagent $Na_2S_2O_8$ are present in the solution, no any $O_2$ evolution is observed under visible light illumination. This result clearly indicates that the POMs starting materials and the ruthenium photosensitizer have no visible-light photocatalytic activity for water oxidation. When the solutions of **POM-1**, **POM-2** and **POM-3** were studied under the same conditions, $O_2$ evolution was investigated from all of them, as shown in Figure 3. The $O_2$ evolution for all three photocatalysts almost linearly increased with irradiation time, indicating that three dye-sensitized POM complexes can be used as stable and efficient water oxidation catalysts (WOCs). The total amount of $O_2$ generated for **POM-1** is about 8.1 μmol after three hours' illumination. The amount of $O_2$ generated for **POM-2** is 44% higher than **POM-1** (11.7 μmol), indicating that $[Mo_5S_2O_{23}]^{4-}$ anion has higher catalytic efficiency for water oxidation than $[Mo_6O_{19}]^{2-}$ cluster. **POM-3** that containing $\alpha$-$[Mo_8O_{26}]^{4-}$ anion displayed the best water oxidation activity xygen evolution since **POM-3** is 2.2 times larger than that for **POM-1** after 3 h illumination. When a longer photoreaction time was performed, the amount of $O_2$ generated for **POM-1**, **POM-2** and **POM-3** after 12 h are 23.7 μmol, 31.6 μmol, and 45.0 μmol, respectively. The $O_2$ evolution results of three complexes showed that the catalytic efficiency of POMs is cluster-size dependent with water oxidation efficiency order: $\alpha$-$[Mo_8O_{26}]^{4-}$ > $[Mo_5S_2O_{23}]^{4-}$ > $[Mo_6O_{19}]^{2-}$. This result is in agreement with the number of Mo = $O_t$ (terminal oxygen) bonds in **POM-3** (14), **POM-2** (10), and **POM-1** (6) because it is well known that the M = $O_t$ bonds are the active sites for photooxidation in POMs-based photocatalysts[25,49,50].

To investigate the catalytic stability of the ruthenium dye-sensitized POM clusters, a three-run test of photocatalytic water oxidation was carried out for **POM-3**, as shown in Figure 4. No additional co-catalyst and sacrificial electron acceptor were added between each run test. There was almost no decrease in the oxygen evolution after three-run test, indicating the quite good stability of **POM-3** as molecular WOCs. The results illustrated that the ruthenium chromophore and POMs hybrid complexes can be used as stable and efficient molecular WOCs. The detailed structures of these complexes could benefit the understanding of water oxidation mechanism for POMs based WOCs and the development of new type POMs-WOCs.

## Discussion

It has been reported that all photocatalytic reactions based on POMs will involve OH· radicals if water is present in reaction systems[25,50]. This finding makes us believe that the possible mechanism of water oxidation in our dye-sensitized POMs is radical cation process.

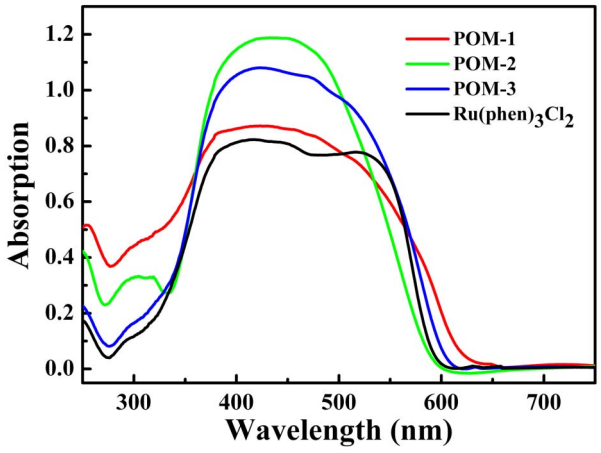


**Figure 2** | **UV-Vis absorption spectra of $Ru(phen)_3Cl_2$, POM-1, POM-2, and POM-3.**

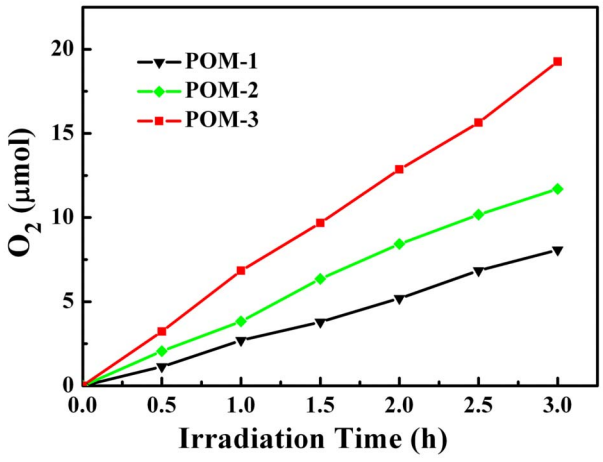


**Figure 3** | **Kinetics of light induced $O_2$ formation from water oxidation with sodium persulfate as a sacrificial electron acceptor for POM-1–3.**

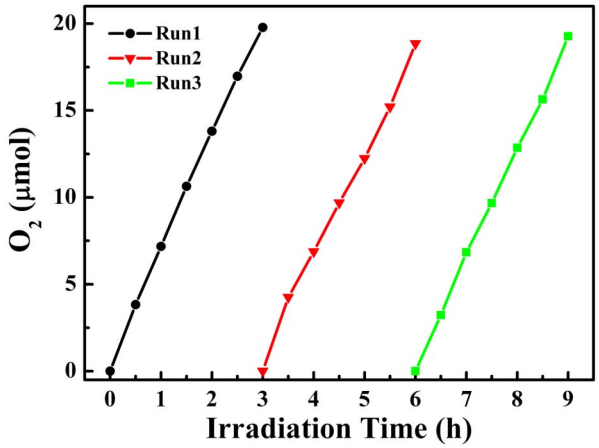


**Figure 4 | Kinetics of light induced $O_2$ formation in the photocatalytic system of POM-3 in the three run test.**

When the ruthenium dye is excited under the visible light, the originally-formed triplet state $[Ru(phen)_3]^{2+}$* is quenched by the $S_2O_8^{2-}$ to form $[Ru(phen)_3]^{3+}$ cation. Then, one electron is transferred from the Mo(VI) = $O_t$ to $[Ru(phen)_3]^{3+}$, resulting in the formation of radical cation Mo(VI) = $O_t^{+}$· and $[Ru(phen)_3]^{2+}$. The radical cation Mo(VI) = $O_t^{+}$· can further oxidize water to produce $O_2$ molecules. The proposed radical cation process is partially confirmed by experimental results. When radical scavenging reagent hydroquinone was added to the solution of **POM-1**, no $O_2$ evolution is observed. HPLC analysis of as-obtained solution showed that *p*-benzoquinone was formed as the oxidation products because hydroquinone can trap OH· radicals (Supplementary Fig. S11)[51].

In conclusion, three new ruthenium dye-sensitized POM hybrid complexes have been successfully synthesized and their structures were determined by single crystal X-ray diffractometer. Although all materials employ the same cation $Ru(phen)_3^{2+}$ as charge-balance species, the anion parts have different size of clusters: $[Mo_6O_{19}]^{2-}$ for **POM-1**, $[Mo_5S_2O_{23}]^{4-}$ for **POM-2**, and α-$[Mo_8O_{26}]^{4-}$ for **POM-3**. Under visible-light illumination, all three complexes show stable $O_2$ evolution with the efficient order **POM-3** > **POM-2** > **POM-1**, which is in agreement with the number order of Mo = $O_t$ (terminal oxygen) groups in clusters because it is well-known that Mo = $O_t$ groups are the catalytically active sites for photooxidation reactions. The possible water-oxidation mechanism is proposed to be radical cation process, which is verified via experimental and theoretical studies. These photocatalysts have been demonstrated to show quite good stability as molecular WOCs. This research could provide a new strategy to develop new POM based WOCs.

## Methods

**Materials.** All chemicals were purchased from Alfa Aesar, TCI chemical and Aldrich and used without further purification. $(TBA)_2[Mo_6O_{19}]$ and a-$(TBA)_4[Mo_8O_{26}]$ were synthesized according to literatures[43,44].

**Synthesis of compound $[Ru(C_{12}N_2H_8)_3CH_3OH][Mo_6O_{19}]$ (POM-1).** $(TBA)_2[Mo_6O_{19}]$ (0.1 mmol, 136 mg) was dissolved into 4 mL of DMF. To the solution, 10 mL of methanol solution containing Dichlorotris(1,10-phenanthroline) ruthenium (II) hydrate (0.1 mmol, 77 mg) was layered on the top in a test tube. Then, the tube was sealed and kept for 10 days. Orange-red crystals were obtained in 85% yield with respect to Ru.

**Synthesis of compound $[Ru(C_{12}N_2H_8)_3][(C_2H_8N_2)_2(C_3H_7NO)]$ $[Mo_5S_2O_{23}]$ (POM-2).** Dichlorotris(1,10-phenanthroline) ruthenium (II) hydrate (0.1 mmol, 72 mg), α-$(TBA)_4[Mo_8O_{26}]$ (0.05 mmol, 108 mg) and sulfur (0.5 mmol, 32 mg) were added to a mixture solution of DMF (4 mL) and acetonitrile (2 mL). The mixture solution was sealed in a Teflon-lined steel autoclave and heating at 110°C for 5 days. The orange-red crystals were isolated after filtration in 52% yield with respect to Ru.

**Synthesis of compound $[Ru(C_{12}N_2H_8)_3CH_3CN]_2[Mo_8O_{26}]$ (POM-3).** The DMF (4 mL) and acetonitrile (2 mL) solution of Dichlorotris(1,10-phenanthroline) ruthenium (II) hydrate (0.2 mmol, 144 mg) and α-$(TBA)_4[Mo_8O_{26}]$ (0.1 mmol, 216 mg) was sealed in a Teflon-lined steel autoclave and heating at 110°C for 5 days. The orange-red crystals were isolated after filtration in 82% yield with respect to Ru.

**Materials characterization.** The optical diffuse reflectance spectra were measured on a PerkinElmer Lambda 750 s UV-Vis spectrometer equipped with an integrating sphere. Powder X-ray diffraction data were recorded on a Bruker D8 Advance diffractometer with a graphite-monochromatized Cu *Ka* radiation. FTIR spectra were recorded from KBr pellets by using a Perkin Elmer FTIR SpectrumGX spectrometer. The quantitative analysis of the product was directly carried out by an Agilent 1100 HPLC using an ultraviolet detector and was determined by inner standard method. A Hypersil ODS (C18) column (4.6 mm 9 5 lm 9 250 mm) was used and the mobile phase was 0.1 M water solution of $H_2SO_4$ DI water at a flow rate of 0.3 mL/min. The column temperature was 40°C and the detection wavelength was 210 nm. The biodiesel samples were diluted with DI water.

**Crystallographic measurements.** Data collection of crystals was carried out on Bruker APEX II CCD diffractometer equipped with a graphite-monochromatized Mo Kα radiation source (λ = 0.71073 Å). Empirical absorption was performed, and the structure was solved by direct methods and refined with the aid of a SHELXTL program package. All hydrogen atoms were calculated and refined using a riding model. The CCDC number for **POM-1**, **POM-2**, and **POM-3** are 900119, 900120, and 900121, respectively.

**Computational methods.** The band structures and DOS of three POM crystals were studied by density functional theory based quantum chemical calculations using Cambridge Series Total Energy Package (CASTEP) program, implemented in the Materials Studio 5.0. Single crystal structural data determined by single-crystal XRD analysis was used to generate the geometries of **POM-1-3**. All the calculations were done using the GGA-PBE functional and ultrasoft pseudo-potentials with a kinetic energy cut off of 300 eV.

**Photocatalytic oxidation of water for $O_2$ generation.** Typically, 10 μmol of the prepared catalysts were suspended in 10 mL aqueous solution of 10 mM $Na_2S_2O_8$. The suspension was purged with argon for 3 h to drive away the residual oxygen before sealed in a quartz flask. The photocatalytic water oxidation was carried out by irradiating the suspension with a 300-W xenon lamp (MAX-302, Asahi Spectra, USA) coupled with a UV cut-off filter (λ > 420 nm). The gas product composition was analyzed every 30 min by an Agilent 7890A gas chromatograph (GC) with TCD detector.


1. Chu, S. & Majumdar, A. Opportunities and challenges for a sustainable energy future. *Nature* **488**, 294–303 (2012).
2. Karunadasa, H. I., Chang, C. J. & Long, J. R. A molecular molybdenum-oxo catalyst for generating hydrogen from water. *Nature* **464**, 1329–1333 (2010).
3. Scholes, G. D., Fleming, G. R., Olaya-Castro, A. & van Grondelle, R. Lessons from nature about solar light harvesting. *Nat. Chem.* **3**, 763–774 (2011).
4. Lewis, N. S. Toward cost-effective solar energy use. *Science* **315**, 798–801 (2007).
5. Narayanam, J. M. R. & Stephenson, C. R. J. Visible light photoredox catalysis: applications in organic synthesis. *Chem. Soc. Rev.* **40**, 102–113 (2011).
6. Xu, X. X., Randorn, C., Efstathiou, P. & Irvine, J. T. S. A red metallic oxide photocatalyst. *Nat. Mater.* **11**, 595–598 (2012).
7. Chen, X. B., Liu, L., Yu, P. Y. & Mao, S. S. Increasing solar absorption for photocatalysis with black hydrogenated titanium dioxide nanocrystals. *Science* **331**, 746–750 (2011).
8. D'Arienzo, M. *et al.* Photogenerated defects in shape-controlled TiO2 anatase nanocrystals: a probe to evaluate the role of crystal facets in photocatalytic processes. *J. Am. Chem. Soc.* **133**, 17652–17661 (2011).
9. Li, Y. F. & Liu, Z. P. Particle size, shape and activity for photocatalysis on titania anatase nanoparticles in aqueous surroundings. *J. Am. Chem. Soc.* **133**, 15743–15752 (2011).
10. Zuo, F. *et al.* Active facets on titanium(III)-doped $TiO_2$: An effective strategy to improve the visible-light photocatalytic activity. *Angew. Chem. Int. Ed. Engl.* **51**, 6223–6226 (2012).
11. Zuo, F. *et al.* Self-doped Ti3+ enhanced photocatalyst for hydrogen production under visible light. *J. Am. Chem. Soc.* **132**, 11856–11857 (2010).
12. Nisar, A. & Wang, X. Surfactant-encapsulated polyoxometalate building blocks: controlled assembly and their catalytic properties. *Dalton Trans.* **41**, 9832–9845 (2012).
13. Cernuto, G., Masciocchi, N., Cervellino, A., Colonna, G. M. & Guagliardi, A. Size and shape dependence of the photocatalytic activity of TiO2 nanocrystals: a total scattering Debye function study. *J. Am. Chem. Soc.* **133**, 3114–3119 (2011).
14. Fang, Y.-H. & Liu, Z.-P. Mechanism and tafel lines of electro-oxidation of water to oxygen on RuO2(110). *J. Am. Chem. Soc.* **132**, 18214–18222 (2010).
15. Li, Y.-F., Liu, Z.-P., Liu, L. & Gao, W. Mechanism and activity of photocatalytic oxygen evolution on titania anatase in aqueous surroundings. *J. Am. Chem. Soc.* **132**, 13008–13015 (2010).

16. Yamazaki, H., Shouji, A., Kajita, M. & Yagi, M. Electrocatalytic and photocatalytic water oxidation to dioxygen based on metal complexes. *Coord. Chem. Rev.* **254**, 2483–2491 (2010).
17. Surendranath, Y., Lutterman, D. A., Liu, Y. & Nocera, D. G. Nucleation, growth, and repair of a cobalt-based oxygen evolving catalyst. *J. Am. Chem. Soc.* **134**, 6326–6336 (2012).
18. Sartorel, A., Carraro, M., Toma, F. M., Prato, M. & Bonchio, M. Shaping the beating heart of artificial photosynthesis: oxygenic metal oxide nano-clusters. *Energy Environ. Sci.* **5**, 5592–5603 (2012).
19. Rivalta, I., Brudvig, G. W. & Batista, V. S. Oxomanganese complexes for natural and artificial photosynthesis. *Curr. Opin. Chem. Biol.* **16**, 11–18 (2012).
20. Liu, X. & Wang, F. Y. Transition metal complexes that catalyze oxygen formation from water: 1979–2010. *Coord. Chem. Rev.* **256**, 1115–1136 (2012).
21. Chen, F. W. & Hu, C. W. Progress in polyoxometalates catalysis. *Prog Chem* **23**, 19–41 (2011).
22. Long, D. L., Tsunashima, R. & Cronin, L. Polyoxometalates: building blocks for functional nanoscale systems. *Angew. Chem. Int. Ed. Engl.* **49**, 1736–1758 (2010).
23. Dolbecq, A., Dumas, E., Mayer, C. R. & Mialane, P. Hybrid organic-inorganic polyoxometalate compounds: from structural diversity to applications. *Chem. Rev.* **110**, 6009–6048 (2010).
24. Proust, A., Thouvenot, R. & Gouzerh, P. Functionalization of polyoxometalates: towards advanced applications in catalysis and materials science. *Chem. Commun.* 1837–1852 (2008).
25. Streb, C. New trends in polyoxometalate photoredox chemistry: From photosensitisation to water oxidation catalysis. *Dalton Trans.* **41**, 1651–1659 (2012).
26. Huang, Z., Geletii, Y. V., Musaev, D. G., Hill, C. L. & Lian, T. Spectroscopic studies of light-driven water oxidation catalyzed by polyoxometalates. *Ind. Eng. Chem. Res.* DOI: 10.1021/ie202950h (2012).
27. Zhang, Z. Y. *et al.* Synthesis and photocatalytic properties of a new heteropolyoxoniobate compound: K-10[Nb2O2(H2O)(2)][SiNb12O40]center dot 12H(2)O. *J. Am. Chem. Soc.* **133**, 6934–6937 (2011).
28. Geletii, Y. V. *et al.* Homogeneous light-driven water oxidation catalyzed by a tetraruthenium complex with all inorganic ligands. *J. Am. Chem. Soc.* **131**, 7522–7523 (2009).
29. Geletii, Y. V. *et al.* An all-inorganic, stable, and highly active tetraruthenium homogeneous catalyst for water oxidation. *Angew. Chem. Int. Ed. Engl.* **47**, 3896–3899 (2008).
30. Yin, Q. S. *et al.* A fast soluble carbon-free molecular water oxidation catalyst based on abundant metals. *Science* **328**, 342–345 (2010).
31. Zhang, Q. C., Wu, T., Bu, X. H., Tran, T. & Feng, P. Y. Ion pair charge-transfer salts based on metal chalcogenide clusters and methyl viologen cations. *Chem. Mater.* **20**, 4170–4172 (2008).
32. Matt, B. *et al.* Hybrid polyoxometalates: Keggin and Dawson silyl derivatives as versatile platforms. *J. Org. Chem.* **76**, 3107–3112 (2011).
33. Matt, B. *et al.* Elaboration of covalently linked polyoxometalates with ruthenium and pyrene chromophores and characteriation of their photophysical properties. *Inorg. Chem.* **50**, 7761–7768 (2011).
34. Zhang, J., Xiao, F. P., Hao, J. & Wei, Y. G. The chemistry of organoimido derivatives of polyoxometalates. *Dalton Trans.* **41**, 3599–3615 (2012).
35. Tran, P. D., Wong, L. H., Barber, J. & Loo, J. S. C. Recent advances in hybrid photocatalysts for solar fuel production. *Energy Environ. Sci.* **5**, 5902–5918 (2012).
36. Kaveevivitchai, N., Chitta, R., Zong, R. F., El Ojaimi, M. & Thummel, R. P. A molecular light-driven water oxidation catalyst. *J. Am. Chem. Soc.* **134**, 10721–10724 (2012).
37. Xu, Y. H. *et al.* Synthesis and catalytic water oxidation activities of ruthenium complexes containing neutral ligands. *Chem. Eur. J.* **17**, 9520–9528 (2011).
38. Puntoriero, F. *et al.* Photoinduced water oxidation using dendrimeric Ru(II) complexes as photosensitizers. *Coord. Chem. Rev.* **255**, 2594–2601 (2011).
39. Yoon, T. P., Ischay, M. A. & Du, J. N. Visible light photocatalysis as a greener approach to photochemical synthesis. *Nat. Chem.* **2**, 527–532 (2010).
40. Car, P. E., Guttentag, M., Baldridge, K. K., Alberto, R. & Patzke, G. R. Synthesis and characterization of open and sandwich-type polyoxometalates reveals visible-light-driven water oxidation via POM-photosensitizer complexes. *Green Chem.* **14**, 1680–1688 (2012).
41. Sartorel, A. *et al.* Water oxidation at a tetraruthenate core stabilized by polyoxometalate ligands: experimental and computational evidence to trace the competent intermediates. *J. Am. Chem. Soc.* **131**, 16051–16053 (2009).
42. Natali, M. *et al.* Photoinduced water oxidation by a tetraruthenium polyoxometalate catalyst: ion-pairing and primary processes with $Ru(bpy)_3^{2+}$ photosensitizer. *Inorg. Chem.* **51**, 7324–7331 (2012).
43. Klemperer, W. G. Tetrabutylammonium isopolyoxometalates. *Inorg. Synth.* **27**, 74–85 (1990).
44. Gao, J. *et al.* Experimental and theoretical studies on pyrene-grafted polyoxometalate hybrid. *Dalton Trans.* **41**, 12185–12191 (2012).
45. Wei, Y. G., Xu, B. B., Barnes, C. L. & Peng, Z. H. An efficient and convenient reaction protocol to organoimido derivatives of polyoxometalates. *J. Am. Chem. Soc.* **123**, 4083–4084 (2001).
46. Li, Q., Wei, Y. G., Wang, Y. & Guo, H. Y. The UV-Vis spectra and substituent effect of organoimido derivatives of polyoxometalates. *Spectrosc. Spect. Anal.* **25**, 923–926 (2005).
47. Besson, C., Chen, S. W., Villanneau, R., Izzet, G. & Proust, A. Chirality of a Strandberg-type heteropolyanion [s2Mo5O23]4−. *Inorg. Chem. Commun.* **7**, 367–369 (2004).
48. Segall, M. D. *et al.* First-principles simulation: ideas, illustrations and the CASTEP code. *J. Phys.: Condens. Matter.* **14**, 2717–2744 (2002).
49. Papaconstantinou, E. Photochemistry of Polyoxometallates of Molybdenum and Tungsten and-or Vanadium. *Chem. Soc. Rev.* **18**, 1–31 (1989).
50. Betley, T. A., Wu, Q., Van Voorhis, T. & Nocera, D. G. Electronic design criteria for O-O bond formation via metal-oxo complexes. *Inorg. Chem.* **47**, 1849–1861 (2008).
51. Bhattacharjee, S. *et al.* Solvothermal synthesis of Fe-MOF-74 and its catalytic properties in phenol hydroxylation. *J Nanosci. Nanotechno.* **10**, 135–141 (2010).

## Acknowledgments

The work is supported by the Singapore National Research Foundation through the Competitive Research Programme under Project No. NRF-CRP5-2009-04 (J.G., Y.Z. and C.X.). Q.Z. acknowledges the financial support from start-up grant (Nanyang Technological University), AcRF Tier 1 (RG 18/09) and Tier 2 (ARC 20/12) from MOE, CREATE program (Nanomaterials for Energy and Water Management) from NRF, and New Initiative Fund from NTU, Singapore. S.C., S.C.J.L. and C.X. thank the support from NTU seed funding for Solar Fuels Laboratory.

## Author contributions

Q.Z. was the overall project leader who initiated the topic and advised on the research. Q.Z. and J.G. wrote the manuscript text. J.G., Y.L., P.C.S.M., L.Y., S.C.J.L. and Y.Z. were responsible for the synthesis and characterization of POM-based photocatalysts. S.C., Q.T., Z.C. and C.X. contributed to the part of water oxidation. K.Y., Y.L. and R.G. were responsible to the part of crystal structure. All authors reviewed the paper.

## Additional information

**Supplementary information** accompanies this paper at http://www.nature.com/scientificreports

**Competing financial interests:** The authors declare no competing financial interests.



**How to cite this article:** Gao, J. *et al.* Molecule-Based Water-Oxidation Catalysts (WOCs): Cluster-Size-Dependent Dye-Sensitized Polyoxometalates for Visible-Light-Driven $O_2$ Evolution. *Sci. Rep.* **3**, 1853; DOI:10.1038/srep01853 (2013).